# Sustainable **Energy & Fuels**



**PAPER** 

View Article Online



Cite this: Sustainable Energy Fuels, 2025. 9. 3014

Received 17th February 2025

Accepted 22nd April 2025 DOI: 10.1039/d5se00246i

rsc.li/sustainable-energy

# Hydrogen bond enhanced electrochemical hydrogenation of benzoic acid over a bimetallic catalyst

Cesar Catizane, Da Ying Jiang\*ab and Joy Sumner\*a

Electrochemical hydrogenation (ECH) is a sustainable alternative to traditional hydrogenation methods, offering selective reduction of organic compounds under mild conditions. This study investigates the cohydrogenation of benzoic acid (BA) and phenol on a platinum-ruthenium on activated carbon cloth (PtRu/ACC) catalyst, with a focus on the synergistic effects arising from hydrogen bonding. Density Functional Theory (DFT) calculations reveal that the formation of a hydrogen-bonded complex between BA and phenol facilitates adsorption energy and lowers activation barrier energies compared to BA alone. Experimental results demonstrate that a 20 mM BA and 5 mM phenol mixture achieves the highest conversion rate (87.33%) and faradaic efficiency (63%), significantly outperforming singlecompound systems. Notably, co-hydrogenation facilitates the reduction of BA to cyclohexanemethanol, a valuable product for biofuel applications, which has reduced corrosiveness and improved energy density. These findings underscore the potential for optimising multi-compound ECH systems through targeted catalyst design and reagent concentration tuning, thus advancing the development of efficient strategies for bio-oil upgrading and sustainable chemical production.

## Introduction

Electrochemical hydrogenation (ECH) has emerged as a promising technology for the selective reduction of organic compounds, offering a cleaner, safer and more energy-efficient alternative to conventional hydrogenation methods. 1-7 By leveraging electrochemical control over hydrogen generation and reaction pathways, ECH allows for precise tunability of products under mild operational conditions. While this method has been extensively studied for single-compound systems, research into the co-hydrogenation of mixed substrates remains limited. Such studies are critical in addressing the complexities found in real-world chemical feedstocks, such as biomass pyrolysis oils, which contain multiple reactive compounds.8 Investigating co-hydrogenation is crucial not only for advancing sustainable chemistry globally but also for optimising processes that deal with complex mixtures in industrial applications. By enabling more efficient, selective transformations, ECH could reduce the need for extensive separation techniques. Thus, research in this area holds significant promise for bridging the gap between laboratory studies and real-world, large-scale applications.

It has been widely reported that the hydrogenation of aromatic compounds follows the Langmuir-Hinshelwood mechanism, that is, the compound/hydrogen interaction happens after both are adsorbed into the surface of a catalytic material.9 This leads to competition for adsorption sites, especially if more than one compound is present simultaneously. Therefore, it is expected that anti-synergistic effects would take place in feedstock which is not pure, lowering the conversion of a particular compound, or all of them. However, previous studies on phenol-containing mixtures (phenol + furfural,10 and phenol + benzaldehyde<sup>11,12</sup>), showed better ECH performances after the addition of phenol, both in terms of conversion rate and selectivity. The authors suggest that a hydrogen-bonded complex formation enhanced the hydrogenation of the coreactant.

In our previous study,13 we demonstrated, for the first time, that a similar synergistic effect seemed to happen during the cohydrogenation of benzoic acid (BA) and phenol, where this mixture led to the increase in both conversion rate and faradaic efficiency, the best results amongst the ones tested. We also found that the hydrogenation of BA, regardless of condition, would lead to a 100% selectivity towards cyclohexane carboxylic acid (CCA), in agreement with Duet al.9 and Fukazawa et al.14

Herein, we explored the interactions between benzoic acid and phenol during the ECH process over a catalyst of platinum ruthenium on activated carbon cloth (PtRu/ACC) for various phenol concentrations, with the aim of better understanding the synergistic effects during co-hydrogenation. Density

<sup>&</sup>lt;sup>a</sup>School of Water, Energy and Environment, Cranfield University, Cranfield, MK43 0AL,  $UK.\ E\text{-}mail:\ ying.jiang@tii.ae;\ j.sumner@cranfield.ac.uk$ 

<sup>&</sup>lt;sup>b</sup>Renewable and Sustainable Energy Research Centre, Technology Innovation Institute, Abu Dhabi, United Arab Emirates

functional theory (DFT) calculations were performed to further elucidate the synergistic hydrogenation mechanism, including nudged elastic bands (NEB), to calculate the activation energy of each step of the hydrogenation and electronic structure calculations, and shed further light on the mechanisms of the reaction.

DFT results show a hydrogen bond enhancement during said process, increasing the adsorption energy of BA, facilitating the reaction and achieving the reduction of BA into cyclohexanemethanol. This novel observation of hydrogen bonds as a catalytic tool represents a significant advancement in the selective hydrogenation process, thus serving as a link between model compound studies and those for whole bio-oil, as well as demonstrating the complex mechanism that takes place during this process.

# Experimental

#### Materials

A sulfuric acid solution (5 M) and benzoic acid (99%, extra pure), were obtained from Thermo Fisher Scientific, while phenol (liquefied, ≥89%) was purchased from Sigma Aldrich. All chemicals were used as received, without any further purification. A Nafion 117 membrane (ion power) was employed as the cation exchange membrane to separate the cathode and anode chambers. To activate the membrane and optimise its ion transport properties, it was pretreated following the method by Peng et al..15 The membrane was treated in hydrogen peroxide (H<sub>2</sub>O<sub>2</sub>) at 80 °C, followed by deionised water and 1.0 M H<sub>2</sub>SO<sub>4</sub> at the same temperature, with each step lasting 1 hour. After each step, the membrane was rinsed with deionised water.

#### **Electrochemical hydrogenation**

A two-chamber electrochemical cell, separated by a proton exchange membrane (PEM), was used for the electrochemical hydrogenation process. The anode consisted of a 1  $\times$  1 cm platinum plate, while the catalytic cathode was a platinum ruthenium black-carbon cloth electrode (Fuel Cell Store, 1:1 Pt: Ru ratio) with a loading of 4 mg cm<sup>-2</sup>. Both chambers were filled with 1.0 M sulfuric acid (H2SO4) as the electrolyte. The ECH tests were conducted in a 90 mL (per chamber) H-type cell, operated under electrostatic control at 25.0 mA cm<sup>-2</sup> and a constant temperature of 55 °C for 10 minutes to polarise the electrodes without the organic compound present. These conditions were established as the optimum conditions for the reaction with BA in our previous study.13

After polarisation, the model compound was introduced to achieve a set final concentration. The electrochemical cohydrogenation of benzoic acid + phenol was carried out at different initial phenol concentrations (5, 10, 15 and 20 mM in 20 mM of BA) to investigate the effect of the presence of said model compound when mixed with benzoic acid (see Table 1). The experiment continued for 4 (for single model compounds experiments) or 5 hours (for mixtures), ensuring the availability of sufficient electrons for compound conversion. Samples (1 mL) were collected every hour, and the organic compounds were extracted with 2 mL of dichloromethane (DCM). NaCl was added until saturation to ensure the migration of the compounds into the DCM. After each experiment, the electrolyte was discarded, the cell was cleaned, and the cathode was soaked in 5 mL of DCM for 15 minutes to desorb any molecules from its surface. All experiments were performed twice, and where there was a standard deviation of more than 5%, a triplicate was carried out.

## Gas chromatography-mass spectrometry (GC-MS)

The samples were analysed in the GC-MS Shimadzu TQ8040. The GC used a Restek Rtx-5 capillary column, 28.5 m  $\times$  0.25 mm with a 0.25 μm film thickness, a 1.18 mL min<sup>-1</sup> helium carrier gas flow rate, and a split ratio of 1:25. The injector temperature was set at 250 °C. The GC oven program started at 34 °C and held for 2 min and then heated at 50 °C min<sup>-1</sup> to 300 °C. Mass spectrometry was operated at m/z ranging from 50 to 500. Species associated with each chromatographic peak were identified by comparing their observed mass spectrum with the NIST library.

#### Calculations

To understand and quantify the ECH process, the following equations were used:

Table 1 Results comparison for the ECH of benzoic acid (BA), phenol (P) and mixtures. Reaction parameters: current density =  $25.0 \text{ mA cm}^{-2}$ , temperature = 55 °C, electrolyte =  $H_2SO_4$  1 M. Where (1) = cyclohexane carboxylic acid, (2) = cyclohexanol, (3) = cyclohexanone, (4) = cyclohexane and (5) = cyclohexanemethanol

Compound initial conc. (mM)				_, ,			Selectivity (%)				
BA	P	Total conversion (%)	BA conversion (%)	Phenol conversion (%)	FE (%)	Space-Time yield (g m <sup>-3</sup> h <sup>-1</sup> )	(1)	(2)	(3)	(4)	(5)
20	_	77.15	77.15	_	56	473.00	100.00	_	_	_	_
20	5	87.33	84.91	97.01	63	505.68	86.38	13.17	0.29	_	0.15
20	10	72.05	62.96	90.23	59	476.23	82.22	17.35	0.43	_	_
20	15	63.92	51.28	80.77	61	478.67	72.57	26.31	1.12	_	_
20	20	66.99	47.35	86.63	75	556.85	65.27	32.55	1.54	0.65	_
_	20	80.75		80.75	64	416.63	_	99.00	1.00	_	_

F.E.(%) = 
$$\frac{\text{mol produced} \times n \times F}{\text{total electrons passed}} \times 100$$
 (1)

$$Conversion(\%) = \left(\frac{\text{moles reactant consumed}}{\text{initial moles reactant}}\right) \times 100 \quad (2)$$

Selectivity(%) = 
$$\left(\frac{\text{moles desired product}}{\text{total moles product}}\right) \times 100$$
 (3)

Current density (mA cm<sup>-2</sup>) = 
$$\frac{\text{current}}{\text{surface area}}$$
 (4)

Space-time yield(g m<sup>-3</sup> h<sup>-1</sup>) = 
$$\frac{\text{mass of product}}{\text{cell volume} \times \text{duration}}$$
 (5)

where F is the Faraday constant (96485 C mol<sup>-1</sup>), and n is the number of electrons necessary for the hydrogenation process (n = 6 for the conversion of benzoic acid into cyclohexane carboxylic acid, for example).

#### **Electrochemical measurements**

Electrochemical measurements were performed using a Palm-Sens EmStat4s at 55 °C, which consisted of a three-electrode system with the selected cathode, anode, and an Ag/AgCl (in saturated KCl solution) as the working, counter, and reference electrodes, respectively. The potential *vs.* Ag/AgCl was converted to the potential *vs.*.RHE (reversible hydrogen electrode) based on the Nernst equation:

$$R_{\text{RHE}} = E_{\text{Ag/AgCl}} + 0.059 \times \text{pH} + E_{\text{Ag/AgCl}^0}$$
 (6)

All electrochemical measurements were carried out in 1.0 M  $\rm H_2SO_4$  with and without the model compounds. Linear scanning voltammetry (LSV) tests were recorded at a scan rate of 5 mV s<sup>-1</sup> from -0.200 V to 0.200 V. Cyclic Voltammetry (CV) was carried out from -0.200 V to 0.200 V, with an  $E_{\rm step}$  of 5 mV and a scan rate of 5 mV s<sup>-1</sup>. Electrochemical Impedance Spectroscopy (EIS) was measured  $\nu s$ . Open Circuit Potential (OCP) at a max frequency of  $10^5$  Hz and a min frequency of  $10^{-1}$  Hz, the  $E_{\rm start}$  was set to -0.200 V. Equilibration time was 5 s.

#### **DFT** calculations

All calculations were carried out using QuantumEspresso/7.2-foss-2022b<sup>16-18</sup> with BURAI 1.3.1 as a visualiser. VESTA was used to calculate the electronic structure. Both positive and negative isosurfaces were set to 0.06 e Å $^{-3}$ . The generalized-gradient approximation (GGA) with the Perdew–Burke–Ernzerhof (PBE) functional described the exchange-correlation energy. To enhance computational performance, all calculations were performed with a thermal smearing of 0.01 Ry and spin polarisation.

A 4-Layer 4  $\times$  4 PtRu (111) slab was built with a 20 Å vacuum gap and two fixed bottom layers. The slab was placed at the bottom of the cell, to certify that all reactions happened on the top surface. A (2  $\times$  2  $\times$  1) k-point grid was set. The test molecule was placed at a distance of 1.5 Å from the surface, where it did not start the calculations with any bonds to the surface.

The adsorption energy  $(E_{\rm ad})$  of the different adsorbates is defined as:

$$E_{\rm ad} = E_{\rm Total} - (E_{\rm adsorbate} + E_{\rm surface}) \tag{7}$$

where  $E_{\text{Total}}$  is the calculated energy for the final system (slab + adsorbate),  $E_{\text{adsorbate}}$  is the calculated energy of each adsorbate and  $E_{\text{Surface}}$  is the energy of the bare cathode surface.

## Results

## Electrochemical co-hydrogenation of benzoic acid and phenol

The impact of phenol concentration on the electrochemical hydrogenation of benzoic acid was systematically investigated, revealing a complex interplay between conversion rates, faradaic efficiency, and space-time yield (STY). ECH of benzoic acid as a stand-alone model compound achieved 77.15% conversion, 56% FE and an STY of 473.00 g m<sup>-3</sup> h<sup>-1</sup> (Table 1). Our previous study<sup>13</sup> demonstrated a direct correlation between FE, STY and initial concentration. By contrast, the correlation between initial concentration and conversion rate is inversely related, that is, increasing initial concentration leads to higher FE, higher STY and lower conversion.

However, the addition of 5 mM of phenol, at a mixture ratio of 20:5, increased all three parameters (conversion = 87.33%, FE = 63% and STY = 505.68 g m<sup>-3</sup> h<sup>-1</sup>). Higher phenol concentrations (20:10 and 20:15) increased FE at the cost of lower STY and conversion rates, at 72.05 and 63.92% conversion and 59 and 61% FE, respectively, when compared to BA alone. Interestingly, the 20:20 mixture increased the conversion rate (66.99  $\nu$ s. 63.92 from the 20:15 mixture) and achieved the highest FE (75%) and STY (556.85 g m<sup>-3</sup> h<sup>-1</sup>). In addition to the total space-time yield reported in Table 1, the yield of cyclohexane carboxylic acid, a product of particular interest, was quantified for each experiment. These values are 473.00, 415.14, 307.80, 250.70, and 231.49 g m<sup>-3</sup> h<sup>-1</sup> for benzoic acid alone, as well as for 20:5, 20:10, 20:15, and 20:20 mixtures, respectively.

At low phenol concentrations, the hydrogen-bonded complex between benzoic acid and phenol stabilises the reactants and facilitates the Langmuir–Hinshelwood mechanism, leading to improved benzoic acid conversion. However, as the phenol concentration increases, the competition for adsorption sites intensifies. Phenol, being more electroactive, outcompetes benzoic acid for active sites on the PtRu/ACC catalyst (see Fig. 3). This results in a noticeable decline in benzoic acid conversion (Fig. 1a), from 84.91 at 5 mM phenol to 62.96, 51.28, and 47.35% at 10, 15 and 20 mM phenol, respectively, where only the 20:5 mixture achieved a higher benzoic acid conversion than BA alone. Despite this, the stronger adsorption of phenol at higher concentrations reduces the likelihood of side reactions such as hydrogen evolution, thereby improving the overall faradaic efficiency and production rate.

Interestingly, the 20:5 and 20:20 ratios exhibit behaviour that deviates from these general trends. At the 20:5 ratio, the synergistic interaction between the two compounds is most pronounced, yielding the highest conversion of benzoic acid. At

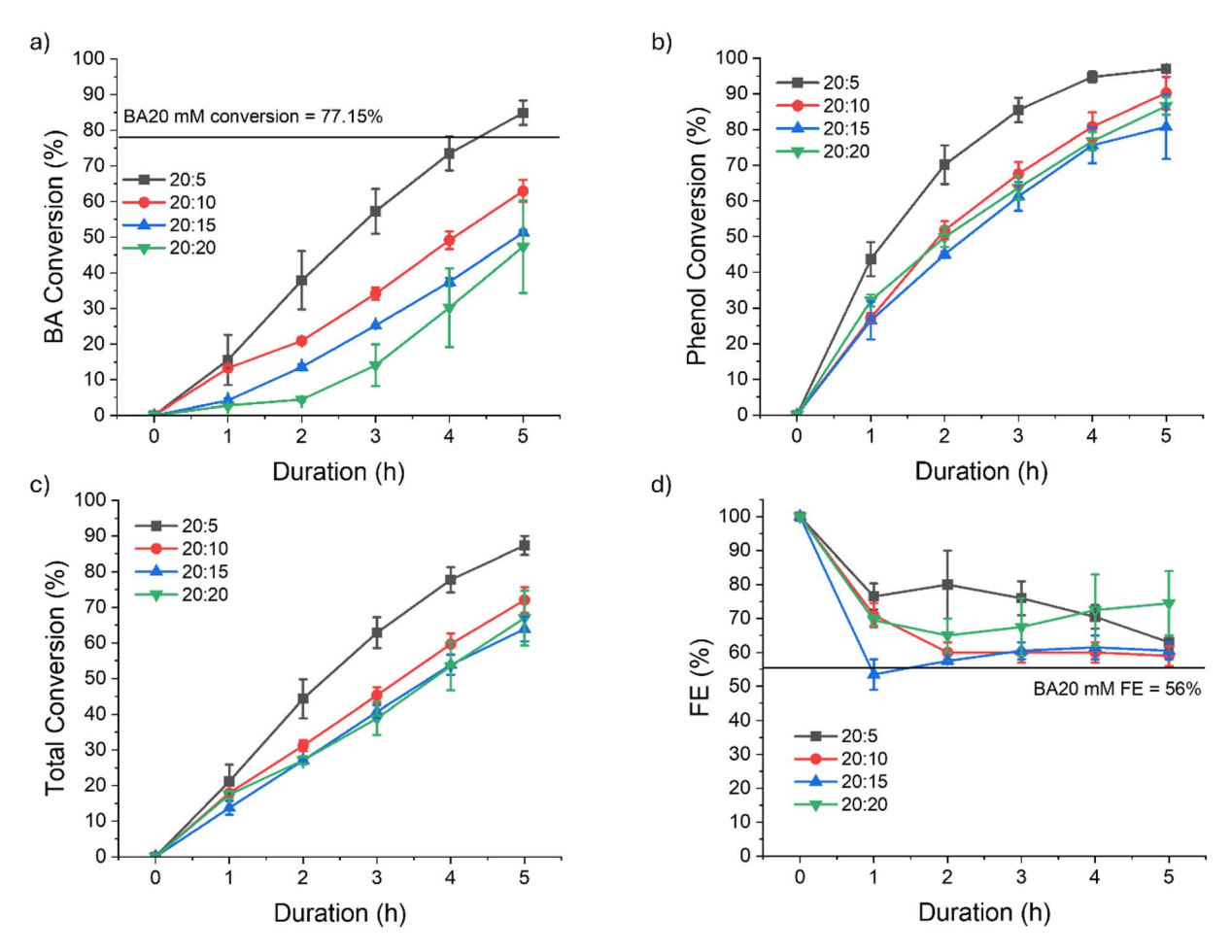


Fig. 1 Co-hydrogenation of benzoic acid (BA) and phenol at various phenol concentrations, the fractions are given by the number in the legend. Where (a) represents the BA conversion, (b) the phenol conversion, (c) the total conversion and (d) represents total FE. Reaction parameters: current density =  $25.0 \text{ mA cm}^{-2}$ , temperature =  $55 \,^{\circ}\text{C}$ , electrolyte =  $H_2 \text{SO}_4 \, 1 \, \text{M}$ . Error bars indicate the standard error of triplicate experimental results.

the 20:20 ratio, despite a reduced conversion of benzoic acid, the system achieves its highest STY and faradaic efficiency. These results suggest that optimal concentrations of phenol depend on the desired outcome: higher conversion rates of benzoic acid are favoured at lower phenol concentrations, whereas higher yields and efficiencies are achieved with a more balanced ratio.

The selectivity of benzoic acid towards cyclohexanemethanol during the co-hydrogenation process is a critical and novel finding of this study. Under most conditions, the reduction of benzoic acid yields cyclohexane carboxylic acid with 100% selectivity, assessed via GC-MS. However, when phenol is present at a 20:5 ratio, the reaction proceeds further, reducing CCA to cyclohexanemethanol. This transformation significantly improves the utility of the product, reducing the corrosiveness of the carboxylic acid group and enhancing the stability, energy density, and C: O ratio of the final mixture, all important factors for the storage, transportation and widespread utilisation of bio-oil in the chemical and biofuel industries.6 The impact of reaction time on conversion rates and product distribution is shown in Fig. 2.

The ability of the reaction to selectively produce cyclohexanemethanol at this ratio is particularly intriguing. It suggests that the phenol concentration not only influences adsorption dynamics but also alters the reaction pathways. The hydrogen-bonded complex formed between phenol and benzoic acid likely plays a key role here, stabilising intermediate states and reducing the energy barrier for the additional hydrogenation step required to convert CCA to cyclohexanemethanol. The DFT calculations corroborate this hypothesis, showing that the presence of phenol decreases the activation energy of key transition states.

The absence of cyclohexanemethanol formation at higher phenol concentrations may reflect the dominance of adsorption site competition under these conditions. At high phenol concentrations, phenol's preferential adsorption over BA limits the availability of active sites for further reducing benzoic acid intermediates. Additionally, the increased adsorption of phenol likely shifts the reaction equilibrium, favouring the production of its own reduction products, such as cyclohexanol and cyclohexanone.

The phenol conversion at the 20:20 ratio demonstrates an intriguing aspect of the synergistic interaction between benzoic acid and phenol during co-hydrogenation. Despite the high

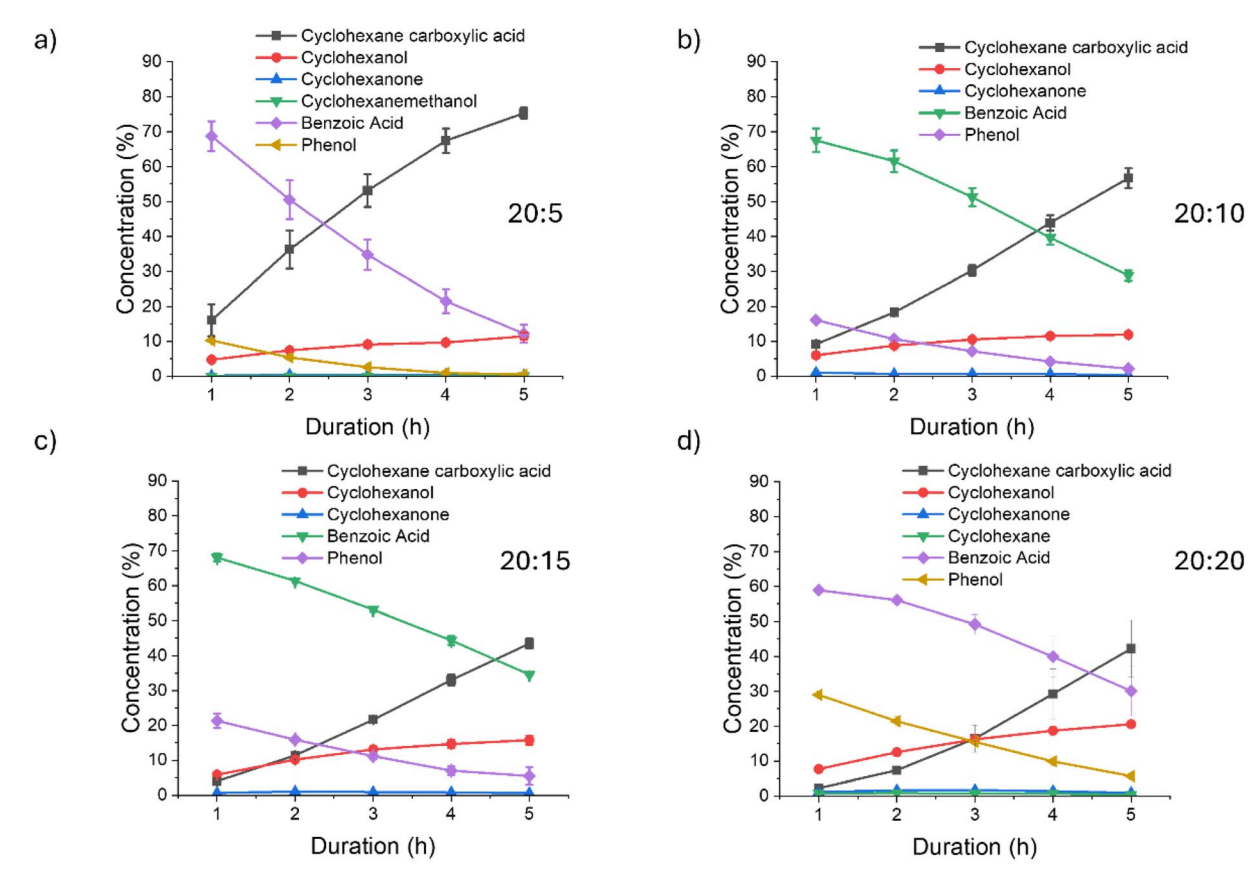


Fig. 2 Impact of reaction time on the co-hydrogenation of benzoic acid and phenol at various phenol concentrations, where (a) represents a benzoic acid: phenol ratio of 20:5, (b) is 20:10, (c) is 20:15 and (d) 20:20. Reaction parameters: current density =  $25.0 \text{ mA cm}^{-2}$ , temperature = 55 °C, electrolyte = H<sub>2</sub>SO<sub>4</sub> 1 M. Error bars indicate the standard error of triplicate experimental results.

concentration of both compounds leading to increased competition for active sites on the PtRu/ACC catalyst, phenol overall conversion remains high, achieving 86.63%. This

a) In the presence of phenol OH OHb) In the presence of benzoic acid +2H+ +2€ +6H+ +6e ₩ H<sub>2</sub>O

Fig. 3 Electrochemical hydrogenation of (a) benzoic acid and (b) phenol. The dashed square shows products that are formed only during the co-hydrogenation of benzoic acid + phenol. (b) Shows two potential routes to the formation of cyclohexanol.

represents an improvement over the conversion of phenol as a stand-alone model compound (80.75%), indicating that the presence of benzoic acid enhances phenol's reduction efficiency under these conditions. The combination of 20 mM of BA and 20 mM of phenol also led to the formation of a different product, cyclohexane. This is probably a product of the hydrogenation of phenol, rather than benzoic acid, which was achieved by increasing the concentration of phenol and focusing on that reaction (Fig. 3b).

## **Electrochemical measurements**

LSV analysis (Fig. 4) shows that PtRu/ACC in the H<sub>2</sub>SO<sub>4</sub> electrolyte exhibits  $-0.1940 \text{ V} \text{ vs. Ag/AgCl at } 10 \text{ mA cm}^{-2}$ , and that it becomes less negative when adding model compounds, reaching -0.1620 V or -0.1590 V vs. Ag/AgCl for 20 mM of BA or phenol, respectively. After the addition of phenol to BA, the potential dislocates to less negative values, reaching -0.1537, -0.1545, -0.1555 and -0.1535 V for 20:5, 20:10, 20:15 and 20:20 mixtures, respectively.

The shift in potential  $(\Delta E)$  reflects two critical phenomena. First, the observed reduction in potential indicates a decrease in competition with the hydrogen evolution reaction (HER), which is mitigated by the presence of phenol, allowing the catalytic sites to focus on the desired hydrogenation reactions.  $\Delta E_1 =$ 

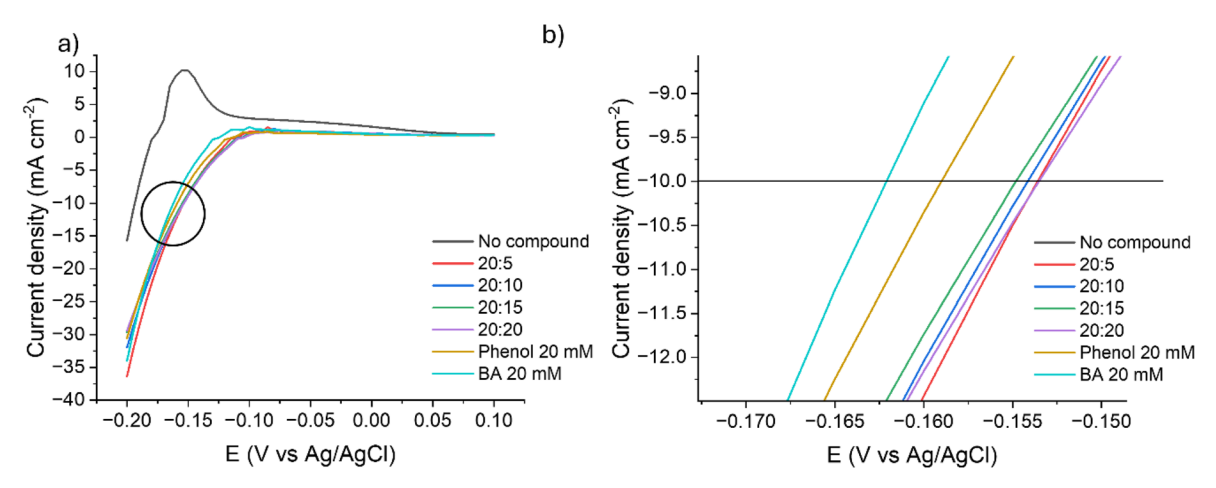


Fig. 4 Linear-sweep voltammetry (a) of PtRu/ACC before (in black) and after the addition of compounds to the electrolyte. Benzoic acid 20 mM (in light blue), phenol 20 mM (in yellow), 20:5 mixture (in red), 20:10 mixture (in blue), 20:15 mixture (in green) or 20:20 mixture (in purple) into the system (1.0 M H<sub>2</sub>SO<sub>4</sub>, 55 °C) and (b) a zoomed-in version to visualise the potential difference at the current density of 10 mAcm<sup>-2</sup>. Where  $\Delta E_1$ ,  $\Delta E_{2}$ ,  $\Delta E_{3}$ ,  $\Delta E_{4}$ ,  $\Delta E_{5}$  and  $\Delta E_{6}$  are the differences between no added compound and BA, phenol, 20:5, 20:10, 20:15 and 20:20 mixtures at 10 mAcm<sup>-2</sup> respectively.

0.032 V and  $\Delta E_2 = 0.035$  V show that the ECH of BA and phenol are favoured when compared to HER, the competing reaction. Second, adding phenol to BA lowers the energy required for ECH, as shown by the  $\Delta E$  values for each mixture. The 20:10 and 20:15 mixtures present an  $\Delta E$  of 0.0395 V and 0.0385 V, respectively. The 20:5 mixture exhibits a higher  $\Delta E$  of 0.0403 V, while the 20:20 mixture shows a slightly larger shift of 0.0405 V. These changes suggest that phenol facilitates the adsorption and activation of hydrogen and benzoic acid on the PtRu/ACC surface. It also supports the claim that the concentrations of 5 and 20 mM of phenol are optimal in this process. Surface characterisation techniques (SEM, XPS, XRD and Raman) were conducted on the PtRu/ACC catalyst and reported in our previous study.13

## Density functional theory calculations

The addition of phenol into the mixture led to the creation of a hydrogen-bonded complex between the alcohol group in phenol and the carboxylic acid in BA (Fig. 5c). The hydroxyl group in phenol interacts with the carboxylic group in benzoic acid,

forming a stable hydrogen-bonded complex. This interaction not only increases the local concentration of reactants near the catalyst surface but also alters the adsorption dynamics. Phenol's hydroxyl group acts as a hydrogen bond donor, while the carboxylic group in benzoic acid serves as an acceptor, redistributing electron density within the molecules. This redistribution makes the aromatic ring of benzoic acid more electrophilic, increasing the likelihood of hydrogen atoms reacting with the carboxyl group and facilitating its reduction. The hydrogen-bonded complex acts as a catalyst, facilitating the cleavage of the double bond O=C leading to the reduction of the carbonyl into an alcohol group, that is, a dehydration reaction.

The charge density difference (Fig. 5) shows an electron accumulation (in yellow) between the molecule and the catalyst surface, with (5b) and without (5a) the addition of phenol, which aligns with the adsorption bonds. Meanwhile, electron depletion (blue areas) around the aromatic ring is larger when phenol is present, indicating a stronger pull of electrons towards the carboxyl group, which makes the phenyl group more positively charged and promotes stronger adsorption.

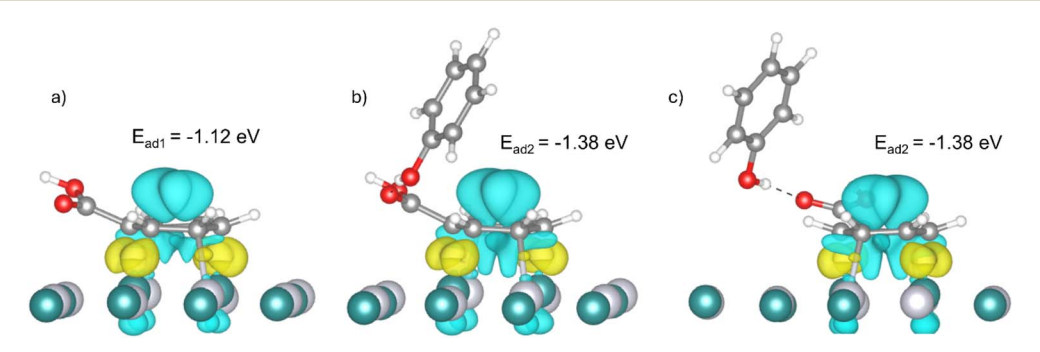


Fig. 5 Charge density difference of benzoic acid adsorbed into PtRu(111) before (a) and after (b) the addition of phenol. The hydrogen-bonded complex is highlighted in a rotated view (c). Electron depletion (light blue) and electron accumulation (yellow) isosurfaces are set to 0.06 e  ${\rm Å}^{-3}$ Where the white spheres represent hydrogen, dark grey is carbon, red is oxygen, light grey is platinum and green represents ruthenium atoms.

These changes in electron density enhance the catalyst's ability to adsorb BA, making the reaction more efficient and lowering the energy required for hydrogenation.

The importance of this enhanced adsorption is highlighted by the adsorption energy  $(E_{\rm ad})$  calculations, which show a significant improvement in adsorption energy from -1.12 eV for benzoic acid alone to -1.38 eV in the presence of phenol. Such a strong interaction stabilises the reactants on the catalyst surface, reducing the likelihood of desorption and enabling more complete hydrogenation.

The results observed in this study align with previous literature reports of synergistic effects in other systems, such as phenol with furfural or benzaldehyde. These studies show that the addition of phenol increased the activity of model compounds for hydrogenation and facilitated selectivity. However, both these compounds are aldehydes that were reduced into alcohols. Therefore, the interaction between benzoic acid and phenol appears particularly effective, forming new and more hydrogenated compounds, reducing oxygen content and saturating all double bonds.

DFT calculations proceeded to identify the reason for the better catalytic effect observed for the mixtures, where the relative energy diagram is shown in Fig. 6. Step-by-step calculation results show that for all intermediate states, that is, every intermediate state of the hydrogenation process, the mixture was more stable than the stand-alone BA. Higher adsorption energies may accelerate and facilitate the adsorption process, which plays a crucial role in the ECH process.

Nudged elastic bands calculations demonstrated that the energy barrier ( $\Delta E$ ) was also reduced when phenol was added. Table 2 shows the variation for each transition state activation energy. The first and fourth steps present the highest activation energies, where  $\Delta E_4$  is the limiting step of the reaction at 1.664 and 1.656 eV for the system without and with phenol, respectively.

The results demonstrate that phenol can not only enhance the adsorption capabilities of benzoic acid but also reduce the activation barrier energies, facilitating the hydrogenation process and enabling the reduction of the carboxylic acid function into alcohol.

Table 2 Activation energy of each step of the hydrogenation process of benzoic acid on PtRu/ACC, before and after the addition of phenol

Step	Energy with no phenol (eV)	Energy with phenol (eV)
$\Delta E_1$	0.983	0.647
$\Delta E_2$	0.599	0.469
$\Delta E_3$	0.367	0.346
$\Delta E_4$	1.664	1.656
$\Delta E_5$	0.232	0.169
$\Delta E_6$	1.014	0.894

The process of BA hydrogenation (Fig. 7) happens with the adsorption of benzoic acid into the surface eqn (8), followed by the Volmer step eqn (9), where an H<sup>+</sup> reacts with an e<sup>-</sup> to produce H\* (adsorbed hydrogen). Subsequently, the H\* transfers into BA\* until the hydrogenation process is completed, and cyclohexane carboxylic acid is produced. The last step is the desorption from the surface eqn (10).

When phenol is added to the mixture, Phenol\* is formed eqn (11), which creates a hydrogen-bonded complex with BA eqn (12). This complex increases the adsorption energy and lowers the activation energy of the hydrogenation process, leading to the reduction of not only the phenyl group, but also the carbonyl group. The final step is the desorption of the cyclohexanemethanol from the surface eqn (13).

The significance of these findings extends beyond the cohydrogenation of benzoic acid and phenol. The ability of phenol to act as a "co-catalyst" by forming hydrogen-bonded complexes could be applied to other bio-oil components with similar functional groups, in concordance with Sanyal *et al.*<sup>10</sup> Moreover, the insights into reduced activation barriers suggest that catalyst design strategies could focus on promoting similar interactions.

These findings have practical implications for the optimisation of ECH processes involving complex feedstocks, such as bio-oils, which often contain phenolic and carboxylic acid compounds. Leveraging the natural synergy between such compounds can reduce energy consumption and improve product selectivity.

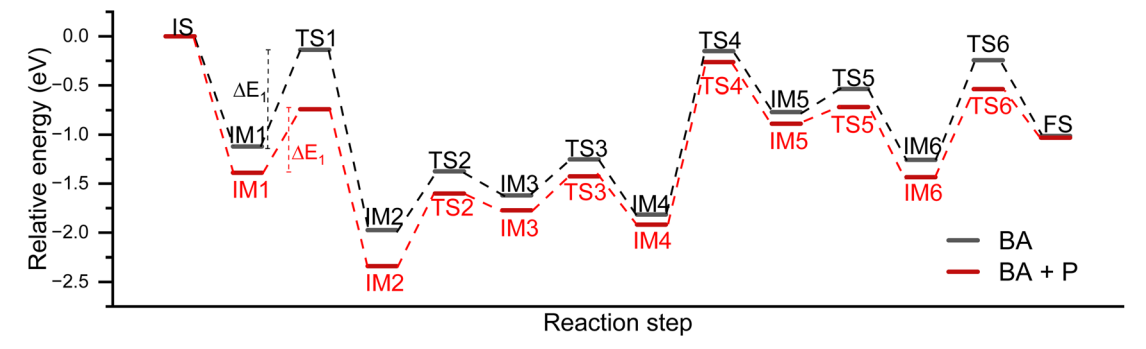


Fig. 6 Relative energy diagram for the ECH of BA (in black) and BA + phenol (in red). Where IS = initial state, IM = intermediate state, TS = transition state and FS = final state. All states are related to the step-by-step hydrogenation of BA.  $\Delta E$  represents the calculated energy barrier for each step.

### ECH mechanism without phenol:

$$(9) \quad H^+ + e^- + * \longrightarrow (H)^{\frac{1}{2}}$$

#### ECH mechanism with phenol:

Proposed mechanism for the ECH of BA over PtRu/ACC before and after the addition of phenol

## Discussion

This study demonstrates the significant impact of hydrogen bond enhancement on the electrochemical co-hydrogenation of benzoic acid and phenol over a platinum-ruthenium catalyst. The formation of hydrogen-bonded complexes between the hydroxyl group of phenol and the carboxyl group of benzoic acid led to stronger adsorption on the catalyst surface, as evidenced by increased electron density and improved adsorption energy. This stronger adsorption enhances the likelihood of hydrogenation, leading to higher conversion rates of benzoic acid.

Moreover, density functional theory calculations confirmed that the addition of phenol reduces the activation energy barriers for the hydrogenation steps. These molecular changes explain the improved efficiency of the co-hydrogenation process, as well as the selectivity for cyclohexanemethanol, which was achieved due to the favourable interaction of the hydrogen-bonded complex with the catalyst. This selectivity is particularly important for bio-oil upgrading, as the formation of alcohols reduces the corrosive effects of carboxylic acids and improves the fuel quality of bio-oil derivatives.

These findings open new avenues for optimising ECH processes, especially for handling complex organic mixtures such as those found in biomass-derived feedstocks. By leveraging hydrogen bond interactions to enhance catalytic efficiency and selectivity, this approach provides a transformative pathway for upgrading bio-oils into higher-value chemical and fuel products. Future research should focus on scaling this process and exploring its potential in real-world biooil systems, where the ability to selectively hydrogenate multiple reactive compounds could revolutionise the production of sustainable fuels and chemicals.

# Data availability

The source data supporting this study's findings are available Figshare repository (https://doi.org/10.6084/ m9.figshare.28398773.v1).

## **Author contributions**

C. Catizane conducted the experimental work and analysis/ imaging and was the primary author of the paper. J. Sumner and Y. Jiang supervised the research, revised the manuscript and contributed to the technical content of the paper.

## Conflicts of interest

There are no conflicts to declare.

# Acknowledgements

The authors wish to thank UK EPSRC (EP/T518104/1) for supporting the work published in the paper through an EPSRC Doctoral Training Partnership Funding.

## References

- 1 R. E. Guedes, A. S. Luna and A. R. Torres, Operating parameters for bio-oil production in biomass pyrolysis: a review, J. Anal. Appl. Pyrolysis, 2018, 129, 134-149.
- 2 Z. Li, Green Chemistry Mild electrocatalytic hydrogenation and hydrodeoxygenation of bio-oil derived compounds using ruthenium supported on activated carbon cloth, Green Chem., 2012, (14), 2540-2549.
- 3 G. Chen, et al., Upgrading of Bio-Oil Model Compounds and Bio-Crude into Biofuel by Electrocatalysis: A Review, ChemSusChem, 2021, 14, 1037-1052.
- 4 R. Kumar and V. Strezov, Thermochemical production of bio-oil: A review of downstream processing technologies for bio-oil upgrading, production of hydrogen and high value-added products, Renewable Sustainable Energy Rev., 2021, 135, 110152.

- 5 I. Graca, J. M. Lopes, H. S. Cerqueira and M. F. Ribeiro, Biooils Upgrading for Second Generation Biofuels, Ind. Eng. Chem. Res., 2012, 52, 275-287.
- 6 S. Hansen, A. Mirkouei and L. A. Diaz, A comprehensive state-of-technology review for upgrading bio-oil renewable or blended hydrocarbon fuels, Renewable Sustainable Energy Rev., 2020, 118, 109548.
- 7 D. Lachos-Perez, et al., Review on Biomass Pyrolysis with a Focus on Bio-Oil Upgrading Techniques, Analytica, 2023, 4, 182-205.
- 8 Q. Zhang, J. Chang, T. Wang and Y. Xu, Review of biomass pyrolysis oil properties and upgrading research, Energy Convers. Manage., 2007, 48, 87-92.
- 9 Y. Du, Electrocatalysis as an efficient alternative to thermal catalysis over PtRu bimetallic catalysts for hydrogenation of benzoic acid derivatives., Green Chem., 2023, 25, 5489-5500.
- 10 U. Sanyal, K. Koh, L. C. Meyer, A. Karkamkar and Simultaneous Y. Gutiérrez, electrocatalytic hydrogenation of aldehydes and phenol over carbonsupported metals, J. Appl. Electrochem., 2021, 51, 27-36.
- 11 L. Liang, et al., Interactions of phenol and benzaldehyde in electrocatalytic upgrading process, Chin. Chem. Lett., 2024, 35, 108581.
- 12 U. Sanyal, et al., Hydrogen Bonding Enhances the Electrochemical Hydrogenation of Benzaldehyde in the Aqueous Phase, Angew. Chem., Int. Ed., 2021, 60, 290-296.
- 13 C. Catizane, Y. Jiang and J. Sumner, Mechanisms of electrochemical hydrogenation of aromatic compound mixtures over a bimetallic PtRu catalyst, Commun. Chem., 2025, 8, 56.
- 14 A. Fukazawa, Y. Shimizu, N. Shida and M. Atobe, Organic & Biomolecular Chemistry Electrocatalytic hydrogenation of benzoic acids in a proton-exchange membrane reactor, Org. Biomol. Chem., 2021, 19, 7363-7368.
- 15 J. Peng, et al., Effect of Boiling Pretreatment on Physicochemical and **Transport Properties** Perfluorosulfonic Acid Membrane, ACS Appl. Polym. Mater., 2023, 5, 9940-9951.
- 16 P. Giannozzi, et al., Quantum ESPRESSO toward the exascale, J. Chem. Phys., 2020, 152, 154105.
- 17 P. Giannozzi, et al., Advanced capabilities for materials modelling with Quantum Espresso, J. Phys.: Condens. Matter, 2017, 29, 465901.
- 18 P. Giannozzi, et al., Quantum espresso: a modular and opensource software project for quantum simulations of materials, J. Phys.: Condens. Matter, 2009, 21, 395502.